Journal of Techniques, ISSN: 2708-8383, Vol. 6, No. 4, 2024, Pages 81-90
DOI: https://doi.org/10.51173/jt.v6i4.2599

JOURNAL OF TECHNIQUES

Journal homepage: http://journal.mtu.edu.iq

RESEARCH ARTICLE - MECHANICAL ENGINEERING

Nonlocal Modeling of Superelastic Behavior in Thin Plate with Central Hole Shape Memory Alloys Under Mechanical Loads

Mohammed Saad Qasim[1*]

[1]Mechanical Engineering Department, Faculty of Engineering and Built Environment, Universiti Kebangsaan Malaysia (UKM), Bangi, Malaysia

[*] Corresponding author E-mail: p121746@siswa.ukm.edu.my

Article Info.

Article history:

Received
01 June 2024

Accepted
17 October 2024

Publishing
31 December 2024

Abstract

Smart metallic materials known as Shape Memory Alloys, or SMAs, have unique deformation attributes, which consist of the shape memory effect as well as superelasticity. In this research, a non-local model of NiTi has been developed to illustrate small-volume SMAs' superelastic behavior. First, an exhaustive overview of the literature was conducted to observe the previous studies on the superelastic behavior of small-volume SMAs and the application of the nonlocal approach in material modeling. Next, a nonlocal model was developed through the Finite Element Method (FEM) to accurately simulate the superelastic effect of small-volume SMAs, accounting for their complicated microstructure and nonlocal effects. The model's accuracy was validated by comparing findings with data from experiments reported in published works. Lastly, the developed nonlocal model is used to study the effects of various parameters, such as the strain rate and the characteristic length scale, on the superelastic behavior of small-volume SMAs. One of the outcomes of this study is introducing a specific finite detail model in the Abaqus R software program, wherein the nonlocal variable works as an extra degree of freedom. This specimen may make the numerical simulation related to the small-volume SMAs' superelastic behavior possible. Additionally, the nonlocal model was validated by comparing its results with data from experiments reported in published works. Moreover, investigating various parameters using the nonlocal model will provide insights into the factors influencing the superelastic behavior of small-volume SMAs under mechanical loads.

Publisher: Middle Technical University

Keywords: SMA; Nonlocal Modeling; Small Volume SMA; Finite Element Model; Superelastic Behavior.

1. Introduction

Shape memory alloys (SMAs) are smart metallic materials with reversible deformation attributes. The SMA's deformation restoration may be classified as superelasticity and the shape memory effect, primarily based on various strategies [1]. The material's potential to regain enormous deformations after heating as an outcome of the temperature-induced degree transformation is called the "shape memory effect". Meanwhile, superelasticity is the material's ability to revert to its preliminary form after being unloaded due to the stress-induced phase transformation. SMAs' particular attributes, like their superelasticity, shape memory effect, good biocompatibility, and high corrosion resistance, make them appealing for diverse uses in biomedicine, aviation, vehicles, civil engineering, aerospace various applications, surgical tools, medical appliance and different industries [1-4]. Superelastic SMAs can be applied as passive control systems in civil engineering, while the shape memory effect in SMAs is commonly used for active control applications Consequently, superelastic SMAs are of significant interest in controlling the seismic response [5,6]. SMA materials are available in various forms, including wires, rods, springs, washers, and plates. Unfortunately, these SMA material compositions are either too costly for large-scale applications or unable to meet the high force capacity requirements of the majority of civil engineering applications. For instance, SMA bars present challenges in machining. When subjected to repeated pressure, the threaded end of the bar is a vulnerable location for initiating cracks, potentially leading to an early fracture. For a fair price, SMA cables composed of multiple SMA wires may offer a sizable force capacity [7]. Effective end anchoring methods for SMA cables were recently designed and tested [8]. As a result, there has been a growing interest in using SMA cables when they are being employed within civil and structural engineering domains to build seismic control systems [9] and isolation systems.

When it comes to dynamics, the nonlocal method is a mathematical and computational technique that takes into account interactions over a limited distance, not only at a single place. It's considered an advanced concept that accounts for the material's mechanical response over a region, leading to more accurate models and better performance predictions in applications involving these unique materials. It reduces numerical dispersion caused by coarse meshes by making model mesh density constraints in spatial domain discretization less stringent [10–13]. Numerical dispersion emerges when the distances between nodes in a model are comparable to the wavelengths. Additionally, nonlocal elasticity through long-range interactions facilitates the formulation of dispersion relationships for arbitrary shapes [14, 15]. There are many applications for nonlocal elasticity in different physical fields, materials, as well as academic domains. Firstly, nonlocal approaches effectively address challenging modeling issues related to geometric discontinuities (e.g., cracks) that pose difficulties for locally formulated classical

Nomenclature & Symbols			
SMA	Shape Memory Alloy	NITI	Nickel Titanium
FEM	Finite Element Method	ZM	Zaki_Moumni Model
NDC	Nitinol Devices & Components	UEL	User Element
LP	Laplacian Operator		

elasticity because of equations based on gradients. Various kinds of geometric discontinuities, such as those brought about by boundary conditions and material nonlinearities, introduce ambiguity in derivative calculations. Nonlocality resolves this by introducing integral-based expressions, reducing or eliminating such inconveniences. Furthermore, nonlocality enables the modelling of spontaneous crack growth in numerical simulations [16,17]. Other applications of nonlocality encompass vibro-acoustic interaction [11], model upscaling [18], regularization of boundary value problems [19], impact loading [20], viscoelasticity [21], thermal diffusion [22], thermoelectricity [23–25], piezoelectricity [26, 27], and the theory of generalized continua for granular media [28]. Nonlocal elasticity has also been successfully applied to model graphene [29, 30] and shape memory alloys (SMAs) [11,31,32]. However, nonlocal modeling is an approach that accounts for the impact of a material's condition over a finite spatial region rather than just at a single point, but it has two disadvantages worth mentioning: the computational costs involved and parameter identification for nonlocal models. Achieving a more reliable material description necessitates an increased number of interactions between body parts and complex material models with coefficients that govern long-range interactions. This leads to more computationally demanding system matrices and comprehensive. The exceptional physical properties of SMAs have enabled various practical applications. Both memory effects and superelasticity are highly desirable attributes that have opened new possibilities for SMA utilization in structures with less stringent requirements regarding movable components, available space, and biocompatibility. Consequently, a novel analytical model has been proposed for superelastic helical SMA springs under axial loading. Here, the model is specifically designed for springs together with an index greater than 4 and a pitch angle greater than 150 degrees, which are frequently used in applications in engineering. It is developed via the ZM constitutive model for SMAs (Zaki and Moumni model, a three-dimensional model of the thermomechanical behaviour of shape memory alloy). The model's major objective is to exactly forecast the helical spring's axial force-deformation relationship whilst accounting for the phase transformation that occur inside the SMA material. By considering this transformation and incorporating the ZM constitutive model, the analytical model gives a comprehensive knowledge of the spring's behaviour. To validate the proposed model, the researchers compared its outcomes with those received from 3-D finite element analysis. This comparison allows the establishment of the accuracy and reliability of the analytical model in describing the complicated conduct of the superelastic helical SMA springs [33].

However, modeling the behavior of SMAs remains a challenging task, specifically while taking into consideration their complex microstructure and the nonlocal nature of the material. The nonlocal method has been shown to be powerful in predicting the behavior of substances with a characteristic length scale [34]. Therefore, in this study, we propose to develop a nonlocal model to simulate the superelastic behavior of SMAs. Then, we aim to compare the results obtained from the nonlocal model with experimental findings available in the literature. We will also investigate the impact of different parameters like the characteristic length scale and the strain rate on the superelastic behavior of small volume thin plate SMAs

2. Methodology

Building on the prevailing body of research, the current investigation is devoted to characterizing the mechanical response of Shape Memory Alloy (SMA) plates under uniaxial deformation. In the first part of the research, a user-defined subroutine referred to as UEL was used to simulate the material response. The subroutine UEL in the Abaqus software program must be used to generate a particular finite element to avail such modeling numerically. The accuracy of the material model is rigorously demonstrated by comparing its predictions with experimental data obtained from NiTi SMA tests, considering that NiTi alloys are regarded as the material of choice for technical applications because of their outstanding functionality and biocompatibility [35]. Subsequently, a detailed analysis was undertaken to model a square plate with a hole. The plate's behavior is systematically explored, first by changing the internal length parameter to recognize its effect. Following this, a comprehensive parametric study was conducted, investigating the influence of hole diameter and plate length on the general responses of the simulated plate while maintaining specified material properties. This established method guarantees a thorough investigation of the SMA plate's mechanical behavior, providing valuable insights into its response under various conditions.

2.1. Model development

The method elucidates the superelastic characteristics underlying the phase transformation. Phase transformation localization and dissemination occur in the presence of persistent stress. To address this, the second gradient implicit technique initially created for damage and nonlocal plasticity has been utilized [36]. The use of this methodology for the localization of phase transformation is also presented in the reference mentioned [37]. Here, we summarize the main equations.

The research conducted by Merzouki [37] demonstrates that the nonlocal volume percentage of the martensite material point can be approximately represented by the following partial differential equation, which is derived from an integral definition.

$$\bar{f}(\vec{\chi}) - l^2\vec{\nabla}^2\bar{f}(\vec{\chi}) = f(\vec{\chi}), \tag{1}$$

where $\vec{\nabla}^2$ Laplacian operator (Lp). It is crucial to observe that the martensite's local volume fraction is of utmost importance, where $f(\vec{\chi})$ represents the origin of the term in the equation for the partial derivative. The parameter symbolizes an internal length parameter that regulates the size of the localization region as well as the interaction range between the material point and its surroundings. The process is completed by implementing a Neumann-type condition on the nonlocal martensite volume fraction at the domain's boundaries. $\Omega\,(\vec{\nabla}\bar{f} = \vec{0}\ on\ \Gamma)$. This boundary condition assumes that the transformation front is constant at the domain boundary. Integrating this condition with Equation (1) leads to the following:

$$\int_\Omega \bar{f}\,(\vec{\chi})d\Omega = \int_\Omega f\,d\Omega \tag{2}$$

This condition indicates that local and nonlocal formulations yield the same martensite in domain Ω. Importantly, contrary to the notion in [34], the deviatoric stress tensor direction does not always orient the martensite local volume fraction.

To account for deformation, the nonlocal formulation modifies the yield transformation force associated with the martensite local volume fraction. The following equation describes how forward or reverse phase transformations develop:

$$\begin{cases} F^{f}_{yield-nonlocal=}F^{f}_{yield}\exp\left(-\frac{H_{\bar{f}}}{H_{\bar{f}}+1}\bar{f}\right) if\ -\dot{f}>0, \\ F^{f}_{yield-nonlocal=}F^{f}_{yield}\exp\left(-\frac{H_{\bar{f}}}{H_{\bar{f}}+1}(1-\bar{f})\right) if\ -\dot{f}<0, \end{cases} \tag{3}$$

Where $H_{\bar{f}}$ is a material parameter factor that regulates the deformation in relation to the nonlocal martensite volume fraction. By using the nonlocal formulation, the state of a material point is contingent upon its internal dynamics and its interaction with its surrounding environment., $\bar{f}$. By using the nonlocal formulation, the state of a material point is contingent upon its internal dynamics and its interaction with its surrounding environment. field Eq. (1) that governs this interaction is specified throughout the whole structure domain; the nonlocal internal variable, $\bar{f}$, is unknown and the scope of the interaction is controlled by the internal length parameter, l.

Equation (4) is numerically solved using the finite element program Abaqus, employing a user-defined subroutine called UEL. The algorithm outlined in (Fig. 1) is implemented in this subroutine, which computes, with regard to degrees of freedom, the updated values of stress, tangent operators Eq. (5), internal variables, residual forces Eq. (4), as well as their derivatives. The integrals required for these calculations are computed using Gauss's method.

$$\begin{cases} \int_{\Omega e}[B^{U}]^{T}\left\{\sum\left(u.\bar{f}\ \right)\right\}d\Omega-\int_{\Gamma_{e}^{\Sigma}}[N^{u}]^{T}\{T^{imposed}\}d\Gamma\ =0 \\ \left(\int_{\Omega e}\left(\left[N^{\bar{f}}\right]^{T}\left[N^{\bar{f}}\right]+\ell^{2}\left[B^{\bar{f}}\right]^{T}\left[B^{\bar{f}}\right]\right)d\Omega\right)\{\bar{f}\}-\int_{\Omega e}\left[N^{\bar{f}}\right]^{T}\ f(u.\bar{f})d\Omega=0 \end{cases} \tag{4}$$

Where Ωe is the finite element volume and Γ_{e}^{Σ} its boundary surface, the corresponding linearized form from Eq. (4) requires the determination of the following tangent operators derived from the nonlocal behavior model

$$H^{uu}=\frac{\partial\Sigma}{\partial E}\ ;\ H^{u\bar{f}}=\frac{\partial\Sigma}{\partial f}\ ;\ H^{\bar{f}u}=\frac{\partial f}{\partial E}\ ;\ H^{\bar{f}\bar{f}}=\frac{\partial f}{\partial f} \tag{5}$$

A customized finite element formulation simulates thin SMA structures subjected to mechanical loads and phase transformation localization. This formula is designed for the numerical modeling of thin SMA structures [38].

The full numerical findings from the simulations have been analyzed in the following part, emphasizing SMA structure behavior and properties under various mechanical stress circumstances.

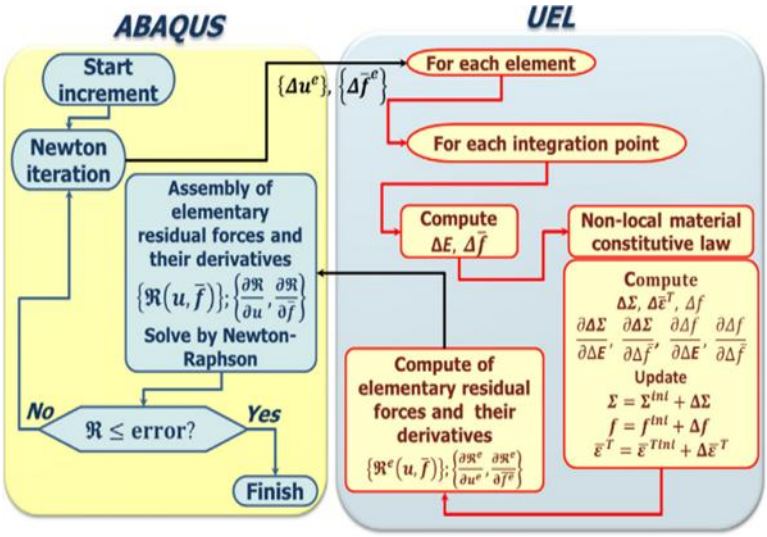

Fig.1. Schematic view of the numerical resolution algorithm implemented in the UEL subroutine [39]

Fig. 2 presents the boundary condition and dimensions of the 2-D simulated SMA plate. On the upper and lower edges of the plate, a simple uniform uniaxial tensile stress is applied in opposite directions.

2.2. Model validation

To validate the model, the material properties were initially confirmed by simulating a standard tensile test based on experimental data. Once the material properties were validated, the model of a square plate was examined. The simulated model was centered around an SMA Nitinol tubing (Ti 49.2 at. %, Ni 50.8 at. %), having a 4.64 mm outer diameter, as well as a 0.37 mm thickness that had been acquired from NDC

(Fremont, CA). In order to test the tubing, specimens measuring 75 mm were made by grinding down the tubing along the test section's 25 mm center. This produced an hourglass-shaped specimen with a 4.3 mm outer diameter. This modification aimed to minimize end effects during testing (as shown in Fig 3). Consequently, pertaining to the gauge section, the wall thickness was decreased to 0.2 mm, generating a roughly 1:10 thickness-to-radius ratio. This meticulous preparation ensured the suitability of the model and its alignment with real-world material properties [40].

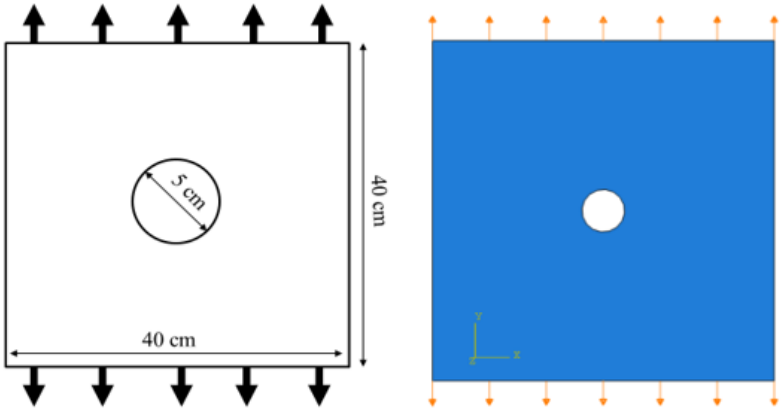

Fig. 2. Schematic diagram of the boundary condition and dimensions of a 2-D SMA plate in tension and its FEM model

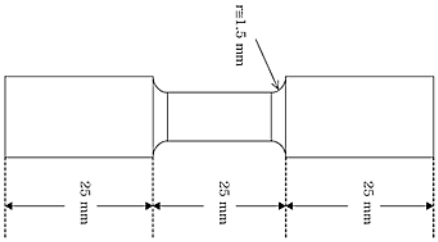

Fig. 3. Dimension of Tensile Specimen [40]

2.3. Sensitivity analysis

To optimize analysis time, mesh sensitivity analyses were performed on a model featuring various simplifications. The finite element model employed in these analyses considered six distinct mesh densities with element sizes across the plate area in increments of 5 mm, 10 mm, 20 mm, 30 mm, 40 mm, and 50 mm. This comprehensive examination aimed to streamline the analysis process while ensuring that the mesh size variations captured the intricacies of the model.

2.4. Parametric study

In the detailed parametric analysis undertaken, several crucial variables had been scrutinized with utmost precision. Specifically, the repercussions of various hole diameters and plate lengths were investigated. This investigative mission delved into a complicated exploration of stress distribution, spanning the complete surface of the plate Each parameter was meticulously tested by exploring a diverse range of values in isolation. This approach facilitated a nuanced and exhaustive exploration of the outstanding effect associated with each parameter being studied.

2.4.1. Effect of hole diameter

An exhaustive analysis was carried out, meticulously studying the effect of 4 discrete hole diameters, particularly 5 cm, 10 cm, 15 cm, and 20 cm. (with a fixed plate length of 40 cm) As the diameter increased progressively, greater stress amplification occurred, highlighting the possibility of local failure.

2.4.2. Effect of plate length

In examining the second parameter of this study, which concentrates on plate length, a comprehensive exploration encompassed four specific values: 40 cm, 60 cm, 80 cm, and 100 cm. For the research of these values, a regular hole diameter of 5 cm was maintained, enabling focused investigations of the impact of different plate lengths on the general structural behavior.

3. Result and Discussion

The findings are systematically categorized based on the main investigations conducted, which consist of analyzing the material response through mechanical cycling. The detected parameters encompass hole diameter and plate length. The overarching goal of this section is to identify and record important material parameters essential for the subsequent computational study. Through a meticulous examination of these various parameters, the focus was on understanding the complex factors governing the mechanical behavior of the material under various conditions, providing a basis for informed analysis and interpretation.

Shape memory nitinol alloy experimental test data was used to determine the material's characteristics. More specifically, the tensile test was used to determine the primary parameters. The procedure involves simulating a tensile test specimen and then validating the results by comparing them with both the model's predictions and the test data. This meticulous comparison ensured the accuracy and reliability of the obtained material properties. Fig. 4 shows the simulated model and its dimensions.

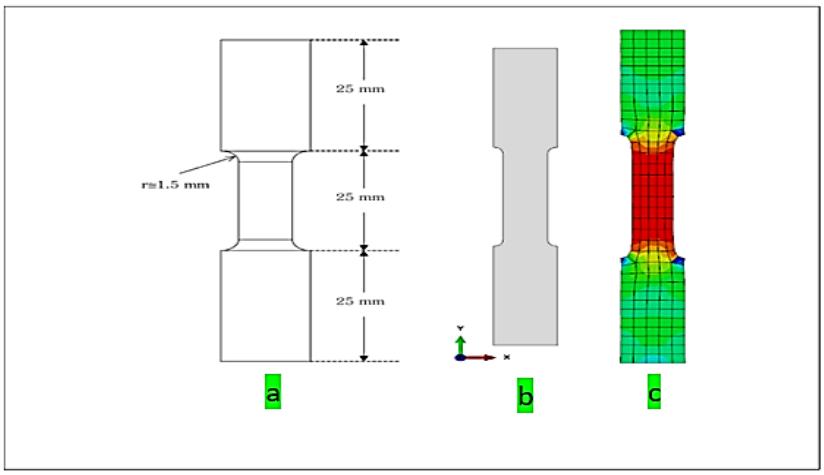

Fig. 4. Tensile test specimen; a) Dimensions of the specimen, b) Simulated specimen, c) Analyzed specimen.

Fig. 5 illustrates a notable alignment between experimental and numerical behaviors. This correspondence indicates that the models effectively capture the material's characteristics, providing an accurate representation. Consequently, these models demonstrate their reliability and suitability for subsequent studies, affirming their potential as tools for further exploration and analysis as shown in detail in Table 1.

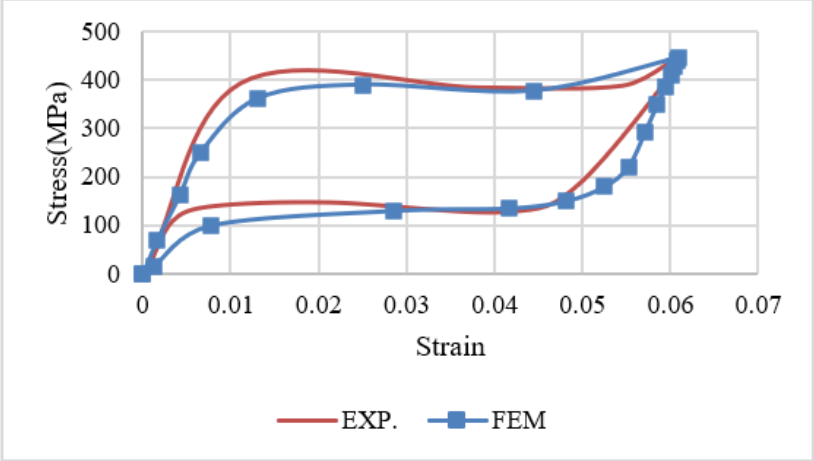

Fig. 5. Comparison between simulated and experimental behaviors of material

Table 1. Comparing the retrieved values for the numerical and experimental models

Strain	EXP. Stress (MPa)	FEM. Stress (MPa)
0.000146	0	0
0.011117	394.0603	362.1077
0.038202	385.195	390.1547
0.054569	388.7411	395.6093
0.060994	441.0461	445.7028
0.04962	185.727	159.6913
0.041344	128.9894	135.4564
0.021273	148.4929	150.6485
0.007829	140.5142	105.4564
0.00335	110.3723	70.1645
0.000243	0.443262	0.011

Mesh sensitivity analyses were conducted using a model with several simplifications, allowing a reduction in analysis time. The finite element model for the mesh sensitivity analyses is illustrated in Fig. 6. Six different mesh densities were examined and included 50, 40, 30, 20, 10 and 5 mm element sizes through the plate area. The same loading conditions were applied for each model. The force-displacement response for each of these models is shown in Fig. 7.

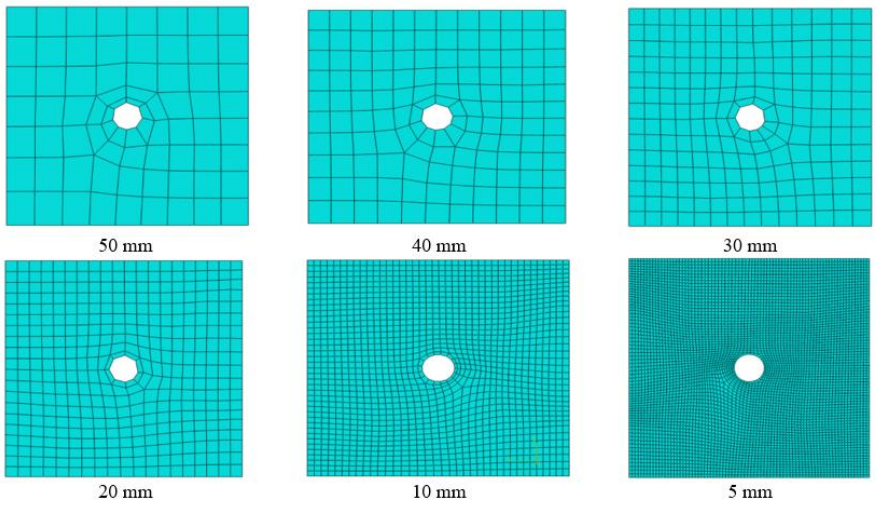

Fig. 6. Finite element models for mesh sensitivity study

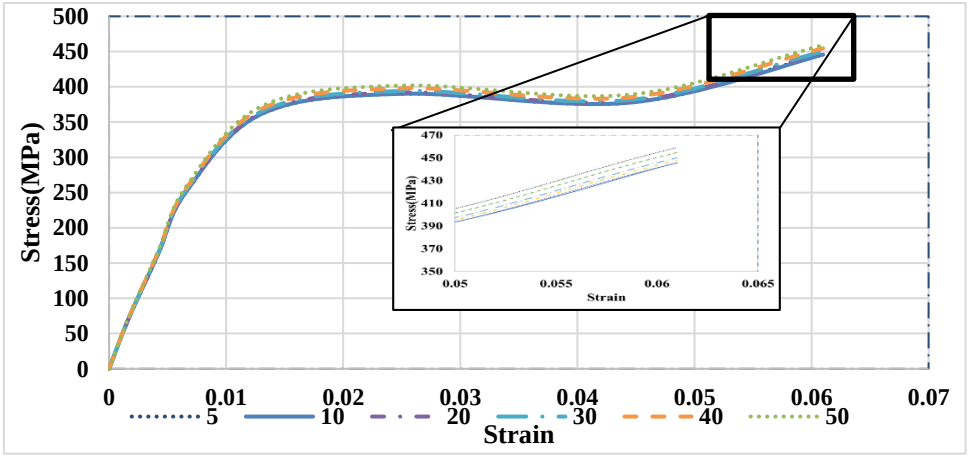

Fig. 7. Stress-strain curves for mesh sensitivity models

In Fig. 7, “stress-strain” refers to the input displacement that is prescribed to the plate. As illustrated by Fig. 7, the stress-strain response for all models is very similar. Referring to the stress-strain response between 350MPa and 470 MPa, the 50-, 40-, 30- and 20-mm mesh size models are still similar to the others, whereas the 10mm and 5mm mesh size models are nearly identical. Approximately 5934 elements were used in the 5mm model, while 1481 were used for the 10mm models. As a result, the 5mm model ran for about 3 times longer than the 10 mm model. Considering the analysis time required and the similarity between the 10mm and 5mm mesh size element models, the 10 mm provided was considered appropriate for providing a representative response. A minimum mesh size is established by this sensitivity analysis, although The results suggest using a finer mesh.

The phenomenon is apparent when the internal length parameter is smaller than the hole size, resulting in a localized phase transformation within the structure. Notably, this localization diminishes entirely as the internal length parameter attains higher values, indicating a homogeneous phase transformation, as shown in Table 2. This approach proves valuable.

For investigating the size effect of a defect within a structure. To further enhance its applicability, a comparison with experimental field measurements is recommended to identify the optimal value for the internal length parameter in a specific material. Furthermore, it is evident that with an increase in strain, higher stresses are generated in the region surrounding the hole. This observation underscores the significance of understanding the relationship between strain levels and stress distribution, providing valuable insights into the mechanical behavior of the material in proximity to the hole.

3.1. Parametric study

In the parametric analysis, two key variables were meticulously examined: the impact of hole diameter and plate length. This investigation is a detailed exploration of stress distribution across the whole of the plate's surface. Each parameter underwent a thorough investigation with a diverse range of values considered independently, rendering a nuanced and exhaustive examination of their respective effects.

3.1.1. Effect of hole diameter

An accurate examination of four distinct hole diameters, 5, 10, 15, and 20 cm, was undertaken. The findings, illustrated in Fig. 8, show that as the hole diameter expands, stress distribution intensifies, mainly towards the corners. This escalating diameter-induced stress amplification heightens the chance of local failure, confirming the critical role of hole size in influencing structural integrity

Table 2. Effect of strain amplitude and internal length parameter on general behavior of the SMA plate

Strain % / ***l***	**5**	**10**	**20**
0	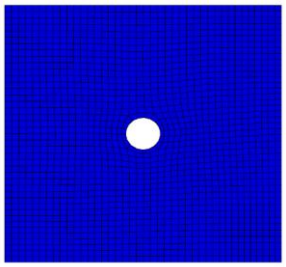	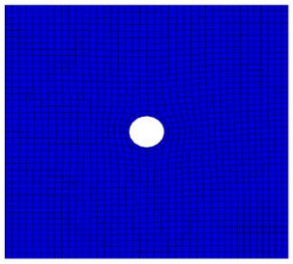	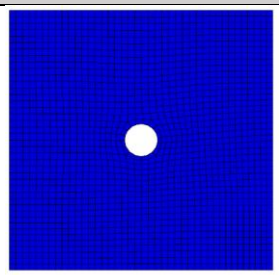
50	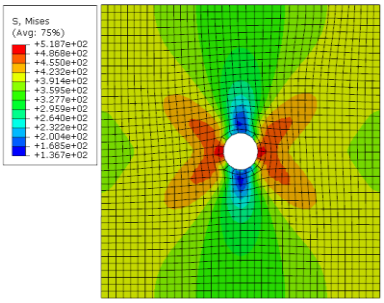	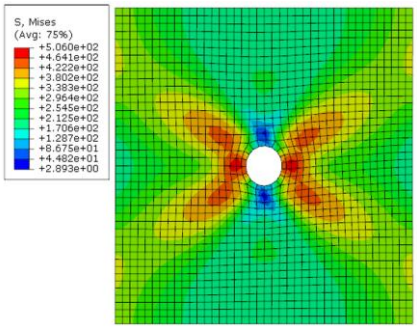	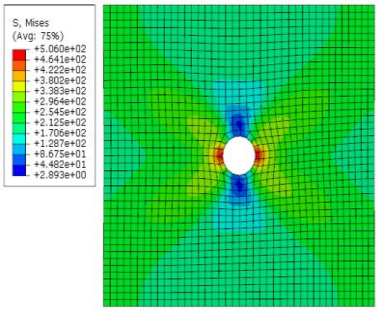
100	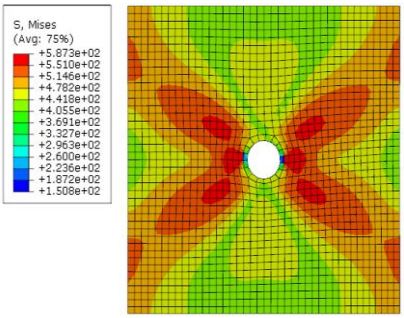	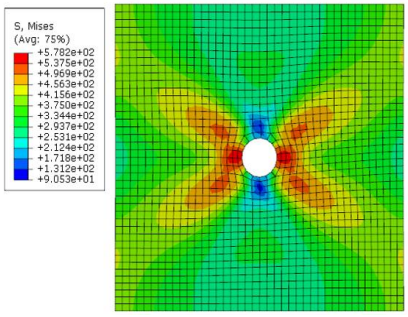	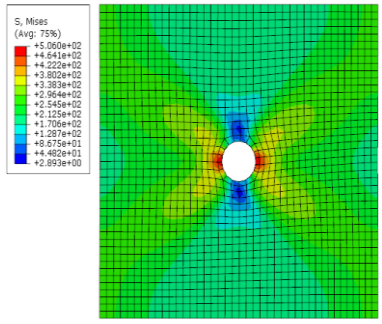

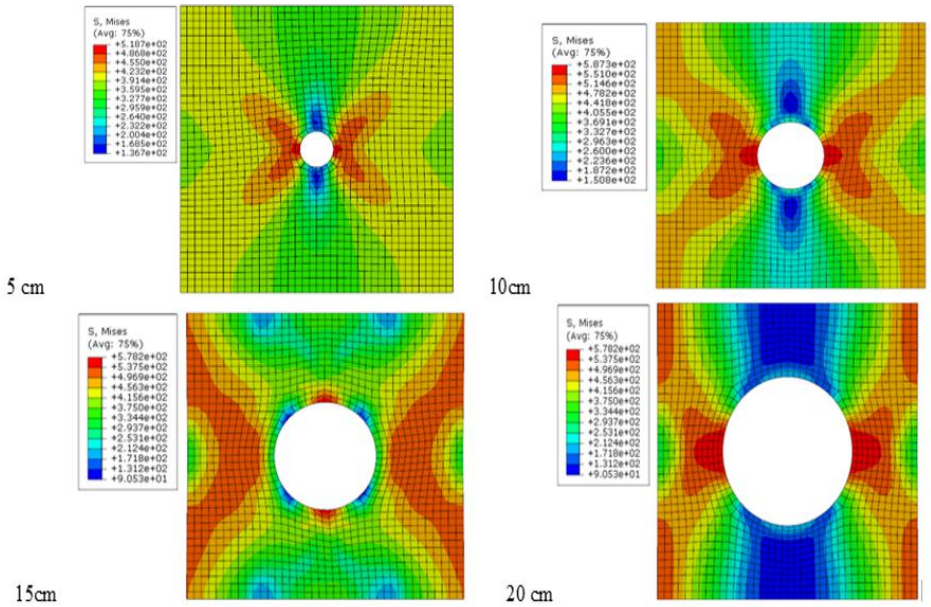

Fig. 8. Effect of hole diameter on the general behavior of the SMA plate

3.1.2. Effect of Plate Length

In examining the second parameter of this study—plate length—four specific values were explored: 40, 60, 80, and 100 cm, with a fixed hole diameter of 5 cm for the investigated values. The insights gleaned from Fig. 9 vividly illustrate a pronounced pattern: as the plate length extends, there is a noteworthy and substantial reduction in stress concentration. This phenomenon is predominantly attributed to the inherent correlation between length and strength, where an increase in length corresponds to an enhancement in structural resilience. This results in a significant decrease in stress concentration.

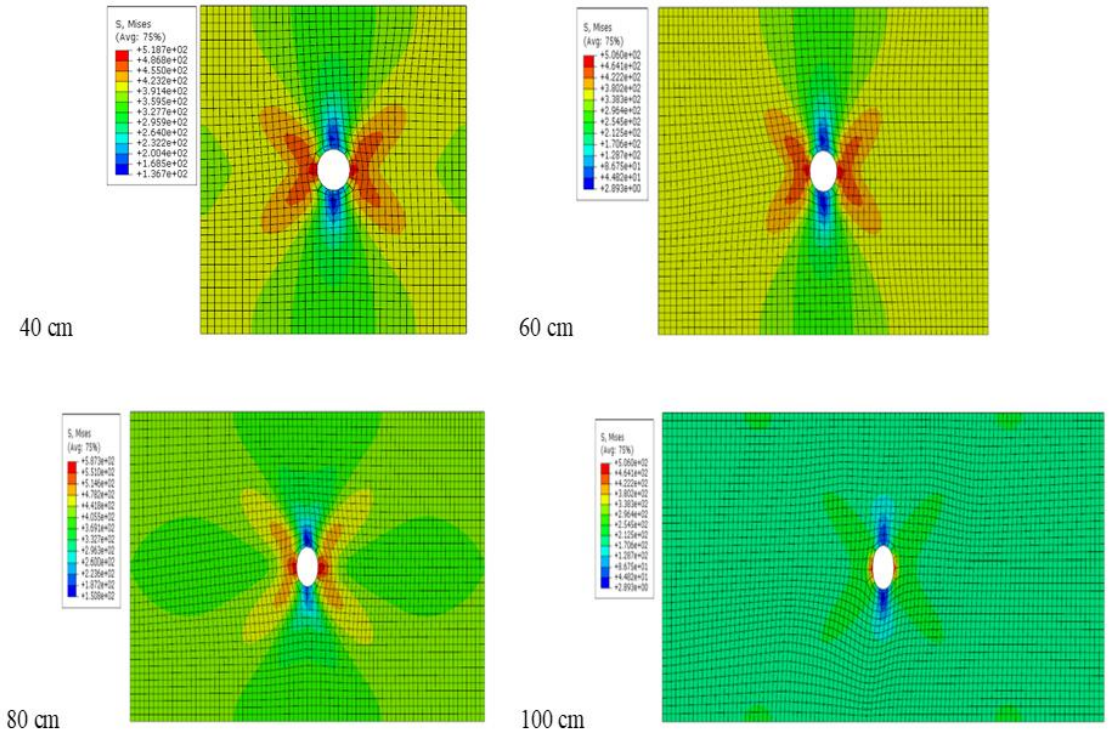

Fig. 9. Effect of plate length on the general behavior of the SMA plate

4. Conclusion

A finite element model, including a nonlocal description related to the martensitic phase transformation, has been established and executed successfully by employing the commercial finite element code Abaqus. This innovative model introduces a crucial internal length parameter that has a close connection to the material's microstructure and allows for the identification of phase transformation localization within thin films. The numerical exploitation of the user subroutine UEL simulations showed an excellent ability to reflect the material's behavior. Whenever the hole size is greater than the internal length parameter, a localized phase transformation within the structure results. Notably, this localization diminishes entirely as the internal length parameter attains higher values, indicating a homogeneous phase transformation. The outcomes showed that mechanical behaviour, regardless of the material's dimensions or properties, involves noticeably distinct features for every change. Also, as the hole diameter expands, stress distribution intensifies, particularly towards the corners. This escalating diameter-induced stress amplification heightens the likelihood of local failure. Finally, there is an inherent correlation between length and strength, where an increase in length corresponds to an enhancement in structural resilience. As the plate length extends, there is a noteworthy and substantial reduction in stress concentration.

Acknowledgment

The authors would like to acknowledge the cooperation and assistance they received from the Technical College of Management - Baghdad, Middle Technical University, Baghdad, Iraq to complete this research.

References

[1] Kröner, E.: “Elasticity theory of materials with long-range cohesive forces.” International Journal of Solids and Structures, 3, 731–742 (1967), https://doi.org/10.1016/0020-7683(67)90049-2.

[2] Ke, Wenchao, et al. “Thermal-fluid behavior, microstructure and mechanical properties in liquid bridge transfer mode during directed energy deposition-arc additive manufacturing–Insights using NiTi as a model alloy.” Additive Manufacturing 77 (2023): 103807. https://doi.org/10.1016/j.addma.2023.103807.

[3] Teshome, Fissha Biruke, et al. “Role of Pd interlayer on NiTi to Ti6Al4V laser welded joints: Microstructural evolution and strengthening mechanisms.” Materials & Design 228 (2023): 111845. https://doi.org/10.1016/j.matdes.2023.111845.

[4] Hussain, Shahadat, et al. “Microstructural and surface analysis of NiTi TPMS lattice sections fabricated by laser powder bed fusion.”

Journal of Manufacturing Processes 102 (2023): 375-386. https://doi.org/10.1016/j.jmapro.2023.07.055.
[5] Kunin, I.A.: "Inhomogeneous elastic medium with non-local interactions." Journal of Applied Mechanics and Technical Physics, 8(3), 60–66 (1967), https://doi.org/10.7494/mech.2015.34.2.41.
[6] Eringen, A.C., Edelen, D.G.B.: "On nonlocal elasticity." International Journal of Engineering Science, 10, 233–248 (1972), https://doi.org/10.1016/0020-7225(72)90039-0.
[7] Martowicz, A.: "On nonlocal modeling in continuum mechanics." Mechanics and Control, 34(2), 41–46 (2015), https://doi.org/10.7494/mech.2015.34.2.41.
[8] Lazar, M., Maugin, G.A. & Aifantis, E.C. 2006. "On a theory of nonlocal elasticity of bi-Helmholtz type and some applications." International Journal of Solids and Structures 43(6), https://doi.org/10.1016/j.ijsolstr.2005.04.027.
[9] Chen, Y., Lee, J.D., Eskandarian, A.: "Atomistic viewpoint of the applicability of microcontinuum theories." International Journal of Solids and Structures, 41, 2085–2097 (2004), https://doi.org/10.1016/j.ijsolstr.2003.11.030.
[10] Singer, I. & Turkel, E. 1998. "High-order finite difference methods for the Helmholtz equation ." Computer Methods in Applied Mechanics and Engineering 163(1–4): 343–358, https://doi.org/10.1016/S0045-7825(98)00023-1.
[11] Martowicz, A., Ruzzene, M., Staszewski, W.J., Rimoli, J.J., Uhl, T.: "Out-of-plane elastic waves in 2D models of solids: a case study for a nonlocal discretization scheme with reduced numerical dispersion." Mathematical Problems in Engineering, Article ID 584081 (2015), https://doi.org/10.1155/2015/584081.
[12] Martowicz, A., Staszewski, W.J., Ruzzene, M., Uhl, T.: "Nonlocal numerical methods for solving second-order partial differential equations." In: Awrejcewicz, J., et al. (eds.) Mathematical and Numerical Aspects of Dynamical System Analysis. 14th Conference Dynamical Systems—Theory and Applications—DSTA 2017, Łód´z, Poland, 11–14 December 2017, pp. 357–368 (2017), https://doi.org/10.1016/j.cma.2019.112621.
[13] Martowicz, A., Ruzzene, M., Staszewski, W.J., Rimoli, J.J., Uhl, T. (2014). " A nonlocal finite difference scheme for simulating wave propagation in reduced numerical dispersion 2D models." In Proceedings of SPIE 9064, Health Monitoring of Structural and Biological Systems 2014, Article ID 90640F, https://doi.org/10.1117/12.2045252.
[14] Martowicz, Adam. 2015. "ON NONLOCAL MODELING IN CONTINUUM MECHANICS." Mechanics and Control 34(2), https://doi.org/10.7494/mech.2015.34.2.41.
[15] Martowicz, Adam, Bryła, J., Staszewski, W.J., Ruzzene, M. & Uhl, T. 2019."Nonlocal elasticity in shape memory alloys modeled using peridynamics for solving dynamic problems." Nonlinear Dynamics 97(3), https://doi.org/10.1007/s11071-019-04943-5.
[16] Prakash, N. & Seidel, G.D. 2018. "Effects of microscale damage evolution on piezoresistive sensing in nanocomposite bonded explosives under dynamic loading via electromechanical peridynamics." Modelling and Simulation in Materials Science and Engineering 26(1), https://doi.org/10.1088/1361-651X/aa938e.
[17] Rodríguez-Ferran, A., Morata, I. & Huerta, A. 2004. "Efficient and reliable nonlocal damage models." Computer Methods in Applied Mechanics and Engineering 193(30–32), https://doi.org/10.1016/j.cma.2003.11.015.
[18] Seleson, P., Parks, M.L., Gunzburger, M., Lehoucq, R.B. (2009). " Peridynamics as an upscaling of molecular dynamics." Journal of Multiscale Modeling & Simulation, 8(1), 204–227, https://doi.org/10.1137/09074807X.
[19] Bazant, Z.P., Jirasek, M. (2002). "Nonlocal integral formulations of plasticity and damage: survey of progress." Journal of Engineering Mechanics, 128(11), 1119–1149, https://doi.org/10.1061/(ASCE)0733-9399(2002)128:11(1119).
[20] Demmie, P.N., Ostoja-Starzewski, M. (2016). "Local and nonlocal material models, spatial randomness, and impact loading." Archive of Applied Mechanics, 86, 39–58, https://doi.org/10.1007/s00419-015-1095-3.
[21] Foster, J.T., Silling, S.A. & Chen, W.W. 2010. " Viscoplasticity using peridynamics." International Journal for Numerical Methods in Engineering 81(10), https://doi.org/10.1002/nme.2725.
[22] Chen, Z. & Bobaru, F. 2015. "Selecting the kernel in a peridynamic formulation: A study for transient heat diffusion." Computer Physics Communications 197, https://doi.org/10.1016/j.cpc.2015.08.006.
[23] Sidhardh, S., Patnaik, S. & Semperlotti, F. 2021. "Thermodynamics of fractional-order nonlocal continua and its application to the thermoelastic response of beams." European Journal of Mechanics - A/Solids 88: 104238, https://doi.org/10.1016/j.euromechsol.2021.104238.
[24] Tuncer, N., Qiao, L., Radovitzky, R. & Schuh, C.A. 2015. "Thermally induced martensitic transformations in Cu-based shape memory alloy microwires." Journal of Materials Science 50(22), https://doi.org/10.1007/s10853-015-9306-4.
[25] Chang, D.M. & Wang, B.L. 2015. "Surface thermal shock cracking of a semi-infinite medium: a nonlocal analysis." Acta Mechanica 226(12), https://doi.org/10.1007/s00707-015-1488-y.
[26] Martowicz, Adam, Kijanka, P. & Staszewski, W.J. 2016. "A semi-nonlocal numerical approach for modeling of temperature-dependent crack-wave interaction. In Health Monitoring of Structural and Biological Systems 2016." Vol. 9805, https://doi.org/10.1117/12.2219148.
[27] Eringen,A.C.1984."Theory of nonlocal piezoelectricity." Journal of Mathematical Physics 25(3), https://doi.org/10.1063/1.526180.
[28] Ebrahimi, F. & Dabbagh, A. 2017. "Wave propagation analysis of embedded nanoplates based on a nonlocal strain gradient-based surface piezoelectricity theory." European Physical Journal Plus 132(11), https://doi.org/10.1140/epjp/i2017-11694-2.
[29] Ostoja-Starzewski, M. 2013. "From random fields to classical or generalized continuum models." In Procedia IUTAM. Vol. 6, https://doi.org/10.1016/j.piutam.2013.01.003.
[30] Arash, B., Wang, Q. & Liew, K.M. 2012. "Wave propagation in graphene sheets with nonlocal elastic theory via finite element formulation." Computer Methods in Applied Mechanics and Engineering 223–224: 1–9, https://doi.org/10.1016/j.cma.2012.02.002.
[31] Duval, Arnaud, Haboussi, M. & Zineb, T. Ben. 2010. "Modeling of SMA superelastic behavior with nonlocal approach. In Physics Procedia." Vol. 10, https://doi.org/10.1016/j.phpro.2010.11.071.
[32] Badnava, H., Kadkhodaei, M. & Mashayekhi, M. 2014. "A nonlocal implicit gradient-enhanced model for unstable behaviors of pseudoelastic shape memory alloys in tensile loading." International Journal of Solids and Structures 51(23–24): 4015–4025, https://doi.org/10.1016/j.ijsolstr.2014.07.021.
[33] Zaki, W. & Viet, N. V. 2018. "Analytical model of shape memory alloy helical springs." In ASME 2018 Conference on Smart Materials, Adaptive Structures and Intelligent Systems, SMASIS 2018. Vol. 1, https://doi.org/10.1115/SMASIS2018-8075.
[34] Chen, Y., Lee, J.D. & Eskandarian, A. 2004. "Atomistic viewpoint of the applicability of microcontinuum theories." International Journal of Solids and Structures 41(8), https://doi.org/10.1016/j.ijsolstr.2003.11.030.
[35] Fazeli, Sara, et al. "Atomistic study of the effect of crystallographic orientation on the twinning and detwinning behavior of NiTi shape

memory alloys." Computational Materials Science 203 (2022): 111080. https://doi.org/10.1016/j.commatsci.2021.111080.

[36] Peerlings, R.H.J., Poh, L.H. & Geers, M.G.D. 2012. "An implicit gradient plasticity-damage theory for predicting size effects in hardening and softening." Engineering Fracture Mechanics 95, https://doi.org/10.1016/j.engfracmech.2011.12.016.

[37] Merzouki, T., Duval, A. & Ben Zineb, T. 2012."Simulation Modelling Practice and Theory 27", https://hal.science/hal-00730848.

[38] Duval, A., Haboussi, M. & Ben Zineb, T. 2011. "Modelling of localization and propagation of phase transformation in superelastic SMA by a gradient nonlocal approach." International Journal of Solids and Structures 48(13): 1879–1893, https://doi.org/10.1016/j.ijsolstr.2011.02.019.

[39] Armattoe, Kodjo Mawuli, Mohamed Haboussi, and T. Ben Zineb. "A 2D finite element based on a nonlocal constitutive model describing localization and propagation of phase transformation in shape memory alloy thin structures." International Journal of Solids and Structures 51.6 (2014): 1208-1220. https://doi.org/10.1016/j.ijsolstr.2013.11.028

[40] McNANEY, James M., et al. "An experimental study of the superelastic effect in a shape-memory Nitinol alloy under biaxial loading." Mechanics of materials 35.10 (2003): 969-986, https://doi.org/10.1016/S0167-6636(02)00310-1.